

Fourier transform algorithms for pricing and hedging discretely sampled exotic variance products and volatility derivatives under additive processes

Wendong Zheng

Department of Mathematics, Hong Kong University of Science and Technology

E-mail: wdzheng@ust.hk

Yue Kuen Kwok*

Department of Mathematics, Hong Kong University of Science and Technology

E-mail: maykwok@ust.hk

* Correspondence author

Keywords: variance products, volatility derivatives, Fourier transform algorithms, additive processes

Date: December 14, 2012

ABSTRACT

We develop efficient fast Fourier transform algorithms for pricing and hedging discretely sampled variance products and volatility derivatives under additive processes (time-inhomogeneous Lévy processes). Our numerical algorithms are non-trivial versions of the Fourier space time stepping method to nonlinear path dependent payoff structures, like those in variance products and volatility derivatives. The exotic path dependency associated with the discretely sampled realized variance is captured in the numerical procedure by updating two path dependent state variables across monitoring dates. The time stepping procedure between successive monitoring dates can be performed using fast Fourier transform calculations without the usual tedious time stepping calculations in typical finite difference algorithms. We also derive effective numerical procedures that compute the hedge parameters of variance products and volatility derivatives. Numerical tests on pricing various variance products and volatility derivatives were performed that illustrate efficiency, accuracy, reliability and robustness of the proposed Fourier transform algorithms.

1 Introduction

Volatility is an important risk measure in managing vega exposure in a portfolio of assets. Also, one may view volatility as the underlying state variable in the asset class of variance products and volatility derivatives. For example, investors can trade on the spread between the realized and implied volatility levels. Unlike equity options, volatility derivatives can provide pure exposure to volatility of the underlying equity. The volatility measure used to define the payoff structures in volatility derivatives may be either the implied volatility derived from option prices or taking the square root of the discretely sampled realized variance obtained by summing the square of the logarithm return of observed asset prices over successive time instants. The trading of volatility derivatives first appeared in 1993 in the form of variance swaps. In the past two decades, we have witnessed the proliferation of different types of variance products and volatility derivatives traded in the financial markets. A recent review of the market for these volatility derivatives can be found in Carr and Lee (2009).

The nonparametric approach of developing various replicating strategies for continuously sampled variance swaps have been proposed in several pioneering works in 1990s. Under the assumption of continuous dynamics of the price process of the underlying stock and existence of the limit of the sum of squared returns, Neuberger (1994) shows that the delta-hedging of a log contract provides a payoff that is related to the variance of the stock's return. Dupire (1993) develops the first preference-free stochastic volatility model that can be used to price

continuously sampled volatility derivatives that are more exotic than the vanilla variance swaps. Carr and Madan (1998) demonstrate how to replicate the payoff of a continuously monitored variance swap by taking a static position in a continuum of options plus dynamic position in the underlying asset. Later works on pricing variance options and volatility derivatives adopt the assumption of jumps in asset returns (Carr *et al.*, 2005) or jumps in both returns and volatility (Sepp, 2008). In more recent works, Kallsen *et al.* (2011) consider pricing options on the quadratic variation of asset return under the affine stochastic volatility model. Drimus (2012) considers pricing and hedging options on continuously sampled realized variance under the non-affine stochastic volatility models and the general class of Log-OU models. Also, Carr *et al.* (2012) consider pricing variance swaps via log contracts under arbitrary exponential Lévy dynamics that is stochastically time-changed by an arbitrary continuous clock.

The contractual specifications of most variance products and volatility derivatives are based on the discretely sampled realized variance of the underlying asset price process. Zhu and Lian (2011) obtain closed form pricing formulas for discretely sampled vanilla variance swaps under stochastic volatility. Zheng and Kwok (2013a) derive pricing formulas for discretely sampled generalized variance swaps, like conditional variance swaps and corridor variance swaps, under the affine stochastic volatility model with simultaneous jumps. They also examine the convergence of the fair strikes of variance swaps under discretely sampled variance to their continuously sampled counterparts [see also a related study by Crosby and Davis (2011)]. Itkin and Carr (2010) obtain closed form pricing formulas of discretely monitored quadratic variation derivatives under a class of Lévy processes with stochastic time change. Broadie and Jain (2008) examine the effect of discrete sampling and asset price jump on the fair strikes of variance and volatility swaps. They show that the well known convexity correction formula may not provide a good approximation of the fair strikes of volatility swaps with jumps in the underlying asset price process. Jarrow *et al.* (2011) examine the sufficient conditions under which the fair strikes of swap products on discretely sampled realized variance converge to those of their continuous counterparts. Keller-Ressel and Muhle-Karbe (2011) propose two methods, one is analytic approximation while the other is exact, for pricing options on discretely sampled realized variance. Zheng and Kwok (2013b) develop the saddlepoint approximation methods for pricing derivatives on discretely sampled realized variance under Lévy models and affine stochastic volatility models. Sepp (2012) analyzes the effect of the discrete sampling on the valuation of options on the realized variance under the Heston stochastic volatility model. He proposes a method that mixes the discrete variance in a log-normal model and the quadratic variation in a stochastic volatility model. Bernard and Cui (2012) study the fair strike of discretely sampled variance swap under a general time-homogeneous stochastic volatility model. They manage to derive asymptotic pricing formulas for the discrete variance swaps.

The analytic derivation of exact or approximation formulas for volatility derivatives under

general type of stochastic processes requires high level of mathematical sophistication and the procedure is invariably quite tedious. In most circumstances, analytic tractability is limited to payoff structures that are mostly linear on quadratic variation of the asset price process. For effective pricing and hedging of volatility derivatives, it would be highly desirable to derive versatile and reliable numerical pricing algorithms for computing prices and their hedge parameters for most types of payoff structures and underlying stochastic price processes.

In this paper, we propose various time stepping algorithms for pricing variance products and volatility derivatives in the Fourier domain. Our fast Fourier transform (FFT) algorithms are distinctive from earlier pricing algorithms that perform numerical calculations in the domain of the original state variable of asset price. Little and Pant (2001) propose a finite difference method for numerical valuation of discretely sampled variance swaps under the local volatility model. Windcliff *et al.* (2006) develop robust numerical schemes that solve the partial integral-differential option pricing equation under jump-diffusion asset price dynamics. The high level of path dependence in discretely sampled volatility derivatives is handled by tracking two stochastic state variables that capture the jump of the sampled variance across a monitoring date. When we consider option pricing under Lévy processes, it is more effective to consider time stepping calculations in the Fourier domain. Lord *et al.* (2008) and Jackson *et al.* (2008) propose effective FFT algorithms for pricing derivatives with mild path dependence in the payoff structures, like the barrier options and American options. A recent review of various FFT algorithms in option pricing under Lévy processes can be found in Kwok *et al.* (2012).

The fast Fourier transform technique can be extended to pricing path dependent options under stochastic volatility, like pricing American options (Zhylyevskyy, 2010) and Bermudan and barrier options (Fang and Oosterlee, 2011). One can also extend the FFT method to time-changed Lévy process by performing appropriate numerical integration over the activity rate dynamics. In this paper, we consider various enhanced versions of the Fourier space time stepping algorithm that extend the class of the underlying price processes to exponential additive processes (time-inhomogeneous exponential Lévy processes) by relaxing the assumption of stationarity of increments in the underlying exponential Lévy processes. Also, the usual requirement of closed form expression for the characteristic function of the underlying asset price process can be relaxed. We simply require the availability of numerical values of the characteristic function at a set of discrete grid points. Our algorithms are constructed to handle exotic path dependence associated with discretely sampled variance (through the incorporation of a set of appropriate jump conditions on the path dependent state variables across monitoring dates). While most analytic approximation formulas in the literature do not include the evaluation of the hedge parameters of the price functions of variance products and volatility derivatives, the set of common hedge parameters like delta and gamma can be computed efficiently using our Fourier transform algorithms. Though our discussion of FFT algorithms is limited to pricing volatility derivatives under the additive process, the pricing

methodologies developed in this paper can be extended at relative ease to other processes like the time-changed Lévy processes and stochastic volatility models. However, these extended versions of FFT algorithms would encounter higher order of computational complexity since additional state variables are included in the pricing models.

The paper is organized as follows. In the next section, we present a brief review of additive processes and the model formulation of discretely sampled variance products and volatility derivatives under additive processes. In Section 3, we first review the FFT algorithms for option pricing using the CONV method (Lord *et al.*, 2008). We then discuss the details of our enhanced FFT pricing algorithms that handle strong path dependence as exhibited in various exotic variance products and volatility derivatives. We also show how to perform the calculations of hedge parameters efficiently. In Section 4, we demonstrate how to compute the fair price functions and their hedge parameters of various types of variance products and volatility derivatives under the piecewise double exponential model (a simple example of an additive process). We report the results from our numerical experiments that were performed to test for accuracy and convergence of the Fourier transform algorithms for pricing different types of variance products and volatility derivatives. Properties on the price functions and hedge parameters of some exotic variance products are also discussed. Conclusive remarks are presented in the last section.

2 Exponential additive processes and derivatives on discretely sampled realized variance

An exponential Lévy process can offer versatile asset return distribution for fitting the actual return distribution and volatility smiles. Equipped with the advantage of nice analytic tractability, Lévy processes have been widely adopted as the underlying asset price processes in pricing various types of exotic derivatives (Carr *et al.*, 2005). However, Lévy processes are well known to have limitations in capturing the term structures of smiles, largely due to the stationarity of increments of Lévy processes. One remedy is to introduce stochastic volatility by time-changing a Lévy process (Carr and Wu, 2004), where the time-changed process is modeled by a non-decreasing process. Under the assumption that the time-changed process is a continuous process, one can introduce an activity rate process that is always positive. In this way, the time-changed process can be represented as an integral of the activity rate process. Though the time-changed Lévy models can fit the volatility smile surface better, an increase in dimensionality adds computational complexity and difficulties in calibration. An alternative approach is to remove stationarity in Lévy processes and take into account deterministic time inhomogeneities (Cont and Tankov, 2003). An advantage of this approach is that most of the nice analytic tractability and computational simplicity of Lévy processes can be carried over

to additive processes. The emphasis of this work is more on the design of FFT algorithms, so we take the class of additive processes as the assumed underlying asset price dynamics in our pricing models of derivatives on discretely sampled realized variance. The numerical pricing methodologies developed in this paper can be extended at relative ease to accommodate more realistic models of asset price dynamics, like stochastic volatility models and time-changed Lévy processes (Fang and Oosterlee, 2011; Itkin and Carr, 2010; Zhylyevskyy, 2012).

Additive processes

A short summary of the properties of additive processes is presented below.

Definition. Let $\mathfrak{B} = (\Omega, \mathcal{F}, (\mathcal{F}_t)_{0 \leq t \leq T}, P)$ be a complete stochastic basis. An additive process is an \mathbb{R} -valued, adapted, càdlàg process $\{X_t : t \geq 0\}$ such that:

1. For any $n \geq 1$ and $0 \leq t_0 < t_1 < \dots < t_n$, the random variables $X_{t_0}, X_{t_1} - X_{t_0}, \dots, X_{t_n} - X_{t_{n-1}}$ are independent.
2. $X_0 = 0$ a.s.
3. X_t is stochastically continuous.

Remark: When the distribution of $X_{t+s} - X_s$ is assumed to be independent of s , the corresponding category of additive processes are known as Lévy processes.

Additive processes belong to a subclass of semimartingales that can be fully characterized by its associated triplet (B, C, ν) of characteristics, where B, C are predictable processes and ν is a predictable random measure on $\mathbb{R}_+ \times \mathbb{R}$. The first characteristic B depends on a truncation function, say, $h(x) = x \mathbf{1}_{\{|x| \leq 1\}}$, which is chosen a priori. A semimartingale is an additive process if and only if its characteristics are non-random.

In practice, the characteristics are usually assumed to be absolutely continuous in time, where

$$B_t = \int_0^t b_s ds, \quad C_t = \int_0^t c_s ds, \quad \nu([0, t] \times G) = \int_0^t F_s(G) ds, \quad \forall G \in \mathcal{B},$$

with predictable processes b, c and a transition kernel F from $(\Omega \times \mathbb{R}_+, \mathcal{P})$ to $(\mathbb{R}, \mathcal{B})$. In this case, we call (b, c, λ) to be the differential characteristics of X . A semimartingale with these differential characteristics resembles locally a Lévy process with triplet $(b, c, F)(\omega, t)$. Hereafter, we implicitly assume (b, c, F) to be a good version in the sense that c_s is nonnegative, $F_s(\{0\}) = 0$ and the triplet satisfies

$$\int_0^T \left(|b_s| + |c_s| + \int_{\mathbb{R}} (1 \wedge |x|^2) F_s(dx) \right) ds < \infty.$$

In the literature, an additive process with absolutely continuous characteristics (also known as an time-inhomogeneous Lévy process) is frequently adopted as the building block for financial modeling (Cont and Tankov, 2003). In financial engineering, the existence of the exponential moments of the driving process is usually required, which naturally leads to the following assumption.

Assumption. *There exists a constant $M > 1$, such that the Lévy measure λ_s satisfies*

$$\int_0^T \int_{\mathbb{R}} \exp(ux) F_s(dx) ds < \infty, \quad \forall u \in [-M, M]. \quad (2.1)$$

Based on the above assumption, by the Lévy-Khintchine formula, the moment generating function is given by

$$e^{\psi_t(u)} = E[e^{uX_t}] = \exp\left(\int_0^t \left[b_s u + \frac{1}{2} c_s u^2 + \int_{\mathbb{R}} (e^{ux} - 1 - ux \mathbf{1}_{\{|x| \leq 1\}}) F_s(dx)\right] ds\right). \quad (2.2)$$

Let $\psi_{t,T}(u)$ denote the cumulant generating function of the increment $X_T - X_t$. By the independency of the increments, we have

$$\begin{aligned} \psi_{t,T}(u) &= \ln E[e^{u(X_T - X_t)}] = \ln \frac{E[e^{uX_T}]}{E[e^{uX_t}]} = \psi_T(u) - \psi_t(u) \\ &= \int_t^T \left[b_s u + \frac{1}{2} c_s u^2 + \int_{\mathbb{R}} (e^{ux} - 1 - ux \mathbf{1}_{\{|x| \leq 1\}}) F_s(dx) \right] ds. \end{aligned} \quad (2.3)$$

Let S_t denote the asset price process with constant dividend yield d and r be the constant riskless interest rate. Suppose the risk neutral dynamics of asset price process is assumed to be an exponential time-inhomogeneous Lévy process under a risk neutral measure Q , where

$$S_t = S_0 e^{(r-d)t} e^{X_t - \psi_t(1)}, \quad t \geq 0. \quad (2.4)$$

Here, X_t is a time-inhomogeneous Lévy process with the triplet of differential characteristics (b, c, F) satisfying the conditions stated above. Note that the compensation term $e^{-\psi_t(1)}$ is appended so that the discounted and dividend-stripped asset price process is a martingale under the risk neutral measure Q .

Derivatives on discretely sampled realized variance

Next, we present the product specifications of various types of derivatives on discretely sampled realized variance. Let $0 = t_0 < t_1 < \dots < t_M = T$ be the monitoring dates for the discretely sampled variance and T be the maturity date. We define $R_m = \ln \frac{S_{t_m}}{S_{t_{m-1}}}$ to be the log return of the underlying asset price over $(t_{m-1}, t_m]$. The discretely sampled realized variance over $[0, T]$

based on the log asset return is defined by

$$\mathbb{V}(0, T; M) = \frac{1}{T} \sum_{m=1}^M R_m^2 = \frac{1}{T} \sum_{m=1}^M \left(\ln \frac{S_{t_m}}{S_{t_{m-1}}} \right)^2. \quad (2.5)$$

The simple asset return is sometimes used as an alternative definition, where the simple asset return is defined by $R_m = \frac{S_{t_m}}{S_{t_{m-1}}} - 1$.

The terminal payoff of the put option, volatility swap and capped variance swap on the discretely sampled realized variance are defined by

$$p(S, \mathbb{V}(0, T; M), T) = \max(K_p - \mathbb{V}(0, T; M), 0), \quad (2.6a)$$

$$w(S, \mathbb{V}(0, T; M), T) = \sqrt{\mathbb{V}(0, T; M)} - K_w, \quad (2.6b)$$

$$V_c(S, \mathbb{V}(0, T; M), T) = \min(\mathbb{V}(0, T; M), C) - K_c \quad (2.6c)$$

respectively, where K_p is the strike of the put option, K_w is the strike of the volatility swap and K_c is the strike of the capped variance swap. The cap C is usually chosen to be some multiple of the fair strike price of the corresponding variance swap without cap. An example of the third generation exotic variance swaps is the downside variance swap. Let U be the specified upper barrier, the discretely sampled downside realized variance is defined by

$$\mathbb{D}(0, T; M, U) = \sum_{m=1}^M \left(\ln \frac{S_{t_m}}{S_{t_{m-1}}} \right)^2 \mathbf{1}_{\{S_{t_m} \leq U\}}, \quad (2.6d)$$

where $\mathbf{1}_{\{\cdot\}}$ is the indicator function. In this corridor-type variance swap, the square of the log asset return over $(t_{m-1}, t_m]$ is counted toward the discretely sampled realized variance only when the asset price S_{t_m} stays at or below the upper barrier U . The corresponding terminal payoff of the downside variance swap is given by $\mathbb{D}(0, T; M, U) - K_d$, where K_d is the strike of the swap.

3 Fourier transform algorithms for pricing variance products and volatility derivatives

Our proposed Fourier transform algorithms for pricing variance products and volatility derivatives are visualized as a synthetic combination of the Convolution (CONV) method (Lord *et al.*, 2008) and the Fourier space time stepping (FST) method (Jackson *et al.*, 2008) for numerical option pricing in the Fourier domain. Also, we adopt the treatment of jump conditions for path dependent state variables in Windcliff *et al.*'s algorithm that deals with the exotic embedded path dependence associated with discretely sampled realized variance. The imple-

mentation of the CONV method requires the conditional probability density of the underlying asset process $f_{X_T|X_t}(y|x)$ to be dependent on x and y only via their difference $y - x$, where

$$f_{X_T|X_t}(y|x) = f_{X_T-X_t}(y-x). \quad (3.1)$$

A sufficient condition for satisfying the above requirement is that the distribution of $X_T - X_t$ is independent of X_t .

FFT technique and CONV method

We perform analytic continuation of w to the complex number field and write $w = \alpha + i\beta$. The generalized Fourier transform \hat{f} of the given function f is defined as follows:

$$\hat{f}(w) = \int_{-\infty}^{\infty} f(x)e^{wx} dx, \quad (3.2a)$$

where α is a constant (known as the damping factor) that is properly chosen to ensure the existence of the generalized Fourier transform \hat{f} . With α being held fixed, the integration with respect to w amounts to integration with respect to β . The Fourier inversion formula can be expressed as

$$f(x) = \frac{1}{2\pi} \int_{-\infty}^{\infty} \hat{f}(w)e^{-wx} d\beta, \quad \text{where } w = \alpha + i\beta. \quad (3.2b)$$

Next, we present a brief discussion of the use of the FFT techniques in the CONV method for pricing European options [refer to Lord *et al.* (2008) and Kwok *et al.* (2012) for details].

Let X_t denote the stochastic process of the underlying stochastic state variable that defines the option payoff. For convenience, we consider the valuation of the undiscounted time- t price function $u(x, t)$ of a European option with the terminal payoff $u(X_T, T)$ at maturity date T , where $X_t = x$. Let $p(x, t; y, T)$ be the transition density from (x, t) to (y, T) . From the renowned Parseval relation in Fourier transform, we have

$$\begin{aligned} u(x, t) &= E_Q[u(X_T, T)|\mathcal{F}_t] \\ &= \int_{-\infty}^{\infty} u(y, T) p(x, t; y, T) dy \\ &= \frac{1}{2\pi} \int_{-\infty}^{\infty} \hat{p}(x, t; w, T) \check{u}(w, T) d\beta. \end{aligned} \quad (3.3)$$

Here, $\hat{p}(x, t; w, T)$ denotes the generalized Fourier transform of $p(x, t; y, T)$ and can be visualized as the conditional moment generating function

$$E_Q[e^{wX_T} | X_t = x] = e^{wx + \psi_{t,T}(w)}.$$

Also, $\check{u}(w, T)$ is defined by

$$\check{u}(w, T) = \check{u}(\alpha + i\beta, T) = \int_{-\infty}^{\infty} e^{-(\alpha+i\beta)y} u(y, T) dy. \quad (3.4)$$

Some special precaution on the choice of α may be required to ensure the existence of $\check{u}(w, T)$.

We may rewrite Eq. (3.3) into the following form:

$$u(x, t) = \frac{e^{\alpha x}}{2\pi} \int_{-\infty}^{\infty} e^{i\beta x} e^{\psi_{t,T}(\alpha+i\beta)} \int_{-\infty}^{\infty} e^{-(\alpha+i\beta)y} u(y, T) dy d\beta, \quad (3.5)$$

Recall that the CONV method can be applied only if the generalized Fourier transform of the terminal payoff function exists. In fact, in order that $\check{u}_T(\alpha + i\beta)$ is finite for all β , the terminal payoff is required to have at least one-sided boundedness with respect to X_T . This requirement is satisfied for equity options with either call-type or put-type payoff function. However, it may become a problem for derivatives on discretely sampled realized variance. This stems from the observation that the realized variance is unbounded when X_T goes to $\pm\infty$ (corresponding to S_T approaching $+\infty$ and 0 , respectively). As a result, the payoff of a variance swap fails to meet this technical requirement of the FFT scheme. Also, there does not exist an appropriate choice of the damping factor α that can ensure the boundedness on both ends. In our calculations, we simply take $\alpha = 0$. To resolve this difficulty in our numerical pricing problems, we impose a cap and floor on the underlying asset price and consider the truncated form of the price function $u(x, t)\mathbf{1}_{|x|\leq L}$ instead of $u(x, t)$. On one hand, the parameter L is chosen to be sufficiently large in order to minimize the approximation error arising from this truncation procedure. On the other hand, L should not be chosen to be too large; otherwise, the discretization error in the FFT calculations would become intolerant. Suppose the computing power allows a sufficiently large value of N (number of grids in the FFT calculations), L can take a large value that is in par with N . This truncation procedure can be justified as follows: given that the resulting expectation value in derivative valuation is finite, the risk neutral density of the asset price distribution should decay faster than any polynomials in X . That is, at a sufficiently large value of X , the value of the density function is close to zero. As a remark, a similar type of truncation in the computational domain is commonly adopted in most numerical option pricing schemes since numerical schemes are operated within the confinement of a finite computational domain.

In the FFT procedure, the Fourier integrals are approximated by a discrete sum via numerical integration quadrature rules. We choose uniform grids for β , x and y , where

$$\beta_n = \beta_0 + n\Delta\beta, \quad x_n = x_0 + n\Delta x, \quad y_n = y_0 + n\Delta y, \quad n = 0, 1, \dots, N-1,$$

with $N = 2^k$ for some positive integer k . It is common to choose $\beta_0 = -\frac{N}{2}\Delta\beta$, $\Delta x = \Delta y$ and

$x_0 = y_0 = -\frac{N}{2}\Delta x$ so that the grids are centered at the origin.

For notational convenience, we write $u(x, t)$ and $\check{u}(w, T)$ as $u_t(x)$ and $\check{u}_T(w)$, respectively. Suppose we approximate the Fourier integrals in Eqs. (3.5) and (3.4) by the trapezoidal rule, we obtain

$$u_t(x_k) = \frac{e^{\alpha x_k}}{2\pi} \sum_{m=0}^{N-1} e^{i\beta_m x_k} e^{\psi_{t,T}(\alpha+i\beta_m)} \sum_{n=0}^{N-1} \gamma_n e^{-i\beta_m y_n} e^{-\alpha y_n} u_T(y_n) \Delta y \Delta \beta, \quad (3.6)$$

where $\gamma_0 = \frac{1}{2}$, $\gamma_{N-1} = \frac{1}{2}$, $\gamma_n = 1$ for $n = 1, 2, \dots, N-2$. We introduce the following notation for the column vector \mathbf{x} :

$$\mathbf{x} = \{x_n\}_{n=0}^{N-1} = (x_0, x_1, \dots, x_{N-1})^T,$$

and let $\mathbf{x} \cdot \mathbf{y}$ denote the element-wise multiplication, where

$$\mathbf{x} \cdot \mathbf{y} = \{x_n y_n\}_{n=0}^{N-1}.$$

In vector forms, the discrete Fourier transform and its inverse transform are denoted by

$$\mathcal{D}(\mathbf{x}) = \left\{ \sum_{n=0}^{N-1} e^{inm2\pi/N} x_n \right\}_{m=0}^{N-1} \quad \text{and} \quad \mathcal{D}^{-1}(\mathbf{x}) = \left\{ \frac{1}{N} \sum_{m=0}^{N-1} e^{-imn2\pi/N} x_m \right\}_{n=0}^{N-1},$$

respectively, where $\mathcal{D}(\mathbf{x})$ and $\mathcal{D}^{-1}(\mathbf{x})$ are column vectors. Taking the usual Nyquist relation:

$$\Delta \beta \Delta x = \frac{2\pi}{N},$$

then Eq. (3.6) can be expressed as

$$u_t(\mathbf{x}) = \mathbf{a} \cdot \mathcal{D}(\mathcal{D}^{-1}(\mathbf{b} \cdot u_T(\mathbf{y}))) \cdot \mathbf{c}, \quad (3.7)$$

where the column vectors \mathbf{a} , \mathbf{b} and \mathbf{c} are defined by

$$\begin{aligned} \mathbf{a} &= \left\{ (-1)^k e^{\alpha x_k} \right\}_{k=0}^{N-1}, \\ \mathbf{b} &= \left\{ (-1)^n \gamma_n e^{-\alpha y_n} \right\}_{n=0}^{N-1}, \\ \mathbf{c} &= \left\{ e^{\psi_{t,T}(\alpha+i\beta_m)} \right\}_{m=0}^{N-1}. \end{aligned}$$

The evaluation of $u_t(\mathbf{x})$ can be efficiently performed via two successive FFT calculations. The CONV method works well provided that the existence of the corresponding generalized Fourier transform is assured.

Path dependence and jump conditions across monitoring dates

We follow the approach in Windcliff *et al.*'s algorithm, where the original multi-state pricing problem is decomposed into a series of one-dimensional model problems indexed by two additional state variables that are updated at discrete monitoring dates.

Let P and Z denote the logarithm of the asset price on the previous monitoring date and the running average of the squared returns accumulated up to the current time, respectively. Apparently, P and Z are only updated on the monitoring dates and stay constant between two consecutive monitoring dates. The updating rules are given by

$$P_{t_m^+} = X_{t_m}, \quad Z_{t_m^+} = Z_{t_m^-} + \frac{R_m^2 - Z_{t_m^-}}{m}, \quad (3.8)$$

where t_m^- and t_m^+ represent the time instant immediately before and after the monitoring date t_m , $m = 1, 2, \dots, M$. We set $P_0 = X_0$ and $Z_0 = 0$. The time- t value of the volatility derivative can be regarded as a function of the logarithm of the underlying asset price X_t and time t . Between two consecutive monitoring dates, the price function $U = U(X, t; P, Z)$ is a function of X and t while the state variables P and Z are treated as parameters.

Time stepping calculations between consecutive monitoring dates

Since P and Z remain constant between two consecutive monitoring dates, the martingale pricing theory gives

$$U(X_{t_{m-1}}, t_{m-1}^+; P, Z) = e^{-r(t_m - t_{m-1})} E[U(X_{t_m}, t_m^-; P, Z) | \mathcal{F}_{t_{m-1}^+}]. \quad (3.9)$$

The numerical calculation of the expectation can be done using the CONV method presented earlier. For the terminal condition, we initiate our time stepping calculations at the instant right before maturity T^- , where

$$U(X, T^-; P_{T^-}, Z_{T^-}) = f\left(\frac{1}{T}[(M-1)Z_{T^-} + (X - P_{T^-})^2]\right) \quad (3.10)$$

for some specified terminal payoff function f .

Jump condition across a monitoring date

Since there is no cash flow to the holder of the derivative across a monitoring date, by no arbitrage argument, the value of the derivative should remain the same at time right before and after any monitoring date t_m . The jump condition is exemplified by

$$U(X, t_m^-; P_{t_m^-}, Z_{t_m^-}) = U(X, t_m^+; P_{t_m^+}, Z_{t_m^+}). \quad (3.11)$$

Backward induction calculations

As in typical option pricing algorithms, we proceed the backward induction calculations from

time t_m to t_{m-1} , $m = M, M - 1, \dots, 1$, until we reach the initiation time t_0 . The price of the derivative on the discretely sampled realized variance at initiation is then obtained.

Choice of the grids

For each state variable, we assign a grid of its respective truncated computational domain. Let N be the number of grid points along the X -grid. We take $\Delta x = L/N$, where L is chosen based on the compromise of truncation error and discretization error. Quite often, some trial and error runs are required to search for the appropriate value of L . By the Nyquist relation, it then follows that $\Delta\beta = 2\pi/L$. For the state variable P , we may assign the same uniform grid as that of X . The determination of the Z -grid is a subtle task. While a fine grid improves accuracy of derivative valuation at the expense of computational cost, it is observed that different types of variance and volatility products may have different sensitivity to the choice of the Z -grid. In our numerical tests, we find that derivatives with linear payoff on the (generalized) realized variance are less sensitive to the Z -grid. When the linear property in the payoff is observed, only two points are needed and the derivative values at some intermediate value of Z can be well estimated by linear interpolation. As a remark, we explain the linear payoff in Z_t for a variance swap as follows. Suppose the current time t lies between t_k and t_{k+1} , the expectation of the discretely sampled realized variance would be given by

$$\sum_{i=1}^k \ln^2 \frac{S_{t_i}}{S_{t_{i-1}}} + E_t \left[\sum_{i=k+1}^n \ln^2 \frac{S_{t_i}}{S_{t_{i-1}}} \right] = kZ_t + E_t \left[\sum_{i=k+1}^n \ln^2 \frac{S_{t_i}}{S_{t_{i-1}}} \right].$$

This illustrates the linear property in the state variable Z_t for a variance swap. However, for nonlinear payoff structures such as volatility swaps and options on discretely sampled realized variance, the distribution of the Z -grid points should be chosen to be sufficiently dense and appropriately placed. To develop the numerical algorithm that is more effective, a nonuniform grid structure (an example is shown in Figure 1) that allocates more points to the left side of the range seems to enhance convergence of the numerical results significantly for pricing put options on discretely sampled realized variance. The possible explanation is that most of the effective contribution to the put option value arises from a very small subinterval of the computational range of Z , within which the option value is significantly different from zero. Essentially, one has to strike a subtle balance between efficiency and accuracy in the choice of nonuniform grids.

Given the grids $\mathbf{x} = \{x_i\}_{i=1}^N$, $\mathbf{p} = \{p_j\}_{j=1}^N$ and $\mathbf{z} = \{z_k\}_{k=1}^K$ for the discretization of X , P and Z , respectively (the adoption of the same uniform grid for \mathbf{x} and \mathbf{p} has been explained earlier), a naive approach would be to compute $U(\mathbf{x}, t_{m-1}^+; p_j, z_k)$ from $U(\mathbf{x}, t_m^-; p_j, z_k)$ via FFT for each pair (p_j, z_k) . This requires the storage of $N^2 \times K$ values in total. When N is large, say $N = 2^{10}$ as a typical level in the actual computation, this requires prohibitively huge memory. We propose an improvement on this memory usage issue by taking advantage of the updating

rule $P(t_m^+) = X_{t_m}$, for $m = 1, \dots, M$. In fact, not each value in these $N^2 \times K$ values obtained in the FFT computation is used to start the next loop. We only need to keep track of those values that correspond to $x_i = p_j$.

The key steps in our FFT algorithm are summarized as follows.

```

For  $m = M$  to 1
  For each  $(p_j, z_k)$ , determine  $U(\mathbf{x}, t_m^-; p_j, z_k)$  using the updating rule Eq. (3.8).
  If  $m = M$ 
    Apply the terminal payoff function in Eq. (3.10) directly
  Else
    Use an interpolation method
  EndIf
  Compute  $U(\mathbf{x}, t_{m-1}^+; p_j, z_k)$  via FFT in Eq. (3.7)
  If  $m = 1$ 
    Output  $U(\mathbf{x}, t_0; P_0, Z_0)$ ; return
  Else
    Store  $U(p_j, t; p_j, z_k)$ 
  EndIf
Next  $j, k$ 
Next  $m$ 

```

Calculations of the hedge parameters

Though the price functions of the derivatives on discretely sampled variance have no dependency on the spot price when evaluated at the initiation date t_0 , the derivative values do have sensitivities with respect to the spot price S_t when we consider the values of in-progress derivatives. Let $t \in (t_{k-1}, t_k]$, where k is fixed, the discretely sampled realized variance on $[0, T]$ can be decomposed into three terms as follows:

$$\mathbb{V}(0, T; M) = \frac{1}{T} \left[\sum_{i=1}^{k-1} \left(\ln \frac{S_{t_i}}{S_{t_{i-1}}} \right)^2 + \left(\ln \frac{S_{t_k}}{S_t} + \ln \frac{S_t}{S_{t_{k-1}}} \right)^2 + \sum_{i=k}^M \left(\ln \frac{S_{t_i}}{S_{t_{i-1}}} \right)^2 \right].$$

The first term is a known quantity by time t with no dependency on S_t while the last term is the future part of the realized variance whose distribution is independent of the spot price under the exponential additive model. The dependency on the spot price stems from the second term. For options on discretely sampled realized variance, the above decomposition cannot be performed due to optionality in the payoff. The CONV method, however, can provide both analytical expressions and numerical schemes for the two important hedge parameters Δ and

Γ as well. For convenience, we write these hedge parameters in terms of the log price X as follows:

$$\Delta = \frac{\partial U}{\partial S} = e^{-X} \frac{\partial U}{\partial X}, \quad \Gamma = \frac{\partial^2 U}{\partial S^2} = e^{-2X} \left(-\frac{\partial U}{\partial X} + \frac{\partial^2 U}{\partial X^2} \right).$$

Since the differentiation can be performed analytically in Eq. (3.5), we have

$$\Delta = \frac{e^{(\alpha-1)x}}{2\pi} \int_{-\infty}^{\infty} e^{i\beta x} (\alpha + i\beta) e^{\psi_{t,T}(\alpha+i\beta)} \check{u}_T(\alpha + i\beta) d\beta, \quad (3.12a)$$

and

$$\Gamma = \frac{e^{(\alpha-2)x}}{2\pi} \int_{-\infty}^{\infty} e^{i\beta x} (\alpha^2 - \alpha - \beta^2 + i(2\alpha - 1)\beta) e^{\psi_{t,T}(\alpha+i\beta)} \check{u}_T(\alpha + i\beta) d\beta. \quad (3.12b)$$

To compute the above greeks, one just need to perform two additional FFTs and inverse FFTs in the final step.

An alternative method is to compute the finite difference approximation of the values of the price function to obtain the values of the hedge parameters. One can make use of the option values at $X = x \pm \Delta x$, which are readily known in the procedure of computing $u(x, t)$, then apply the standard centered finite difference approximation formulas:

$$\Delta = \frac{u(x + \Delta x, t) - u(x - \Delta x, t)}{2\Delta x}, \quad (3.13a)$$

$$\Gamma = \frac{u(x + \Delta x, t) - 2u(x, t) + u(x - \Delta x, t)}{\Delta x^2}. \quad (3.13b)$$

4 Numerical examples

In this section, we report the numerical tests that were performed using our proposed FFT algorithms for computing the price functions and their hedge parameters of various variance and volatility products under a “piecewise” double exponential model.

Piecewise double exponential model

In our sample calculations, we take the underlying asset price process to follow the piecewise double exponential model, chosen as a simple example of Lévy process with time inhomogeneity. A “piecewise” double exponential model is constructed by modeling the underlying asset price process with different double exponential models over different time intervals. Consider a typical “piece” of the piecewise double exponential model over a specified time interval within

the life of the derivative, the risk neutral dynamics of the asset price S_t observes the following jump diffusion process of double exponential type:

$$\frac{dS_t}{S_t} = (r - d - m\lambda)dt + \sigma dW_t + (e^Y - 1) dN_t, \quad (4.1)$$

where N_t is a Poisson process with intensity λ that is independent of W_t , and Y denotes the independent random jump size and has an asymmetric double exponential distribution specified by

$$Y = \begin{cases} \xi_+ & \text{with probability } p \\ -\xi_- & \text{with probability } 1 - p \end{cases}.$$

Here, ξ_{\pm} are exponential random variables with means $1/\eta_{\pm}$, respectively; and

$$\begin{aligned} m &= E[e^Y - 1] \\ &= p \left(\int_0^{\infty} \eta_+ e^{-(\eta_+ - 1)y} dy - 1 \right) + (1 - p) \left(\int_0^{\infty} \eta_- e^{-(\eta_- + 1)y} dy - 1 \right) \\ &= \frac{p}{\eta_+ - 1} - \frac{1 - p}{\eta_- + 1}. \end{aligned}$$

For simplicity, we adopt the two-piece double exponential model. We assume the asset price process to follow a double exponential jump diffusion process on $[0, t_0]$ and another double exponential jump diffusion process with a different set of parameters on $(t_0, T]$. The combination of these two pieces of separate double exponential jump diffusion processes is a time-inhomogeneous Lévy process.

t	σ	λ	η_+	η_-	p
$[0, 0.05]$	0.3	3.97	16.67	10	0.15
$(0.05, T]$	0.18	1.43	10	6.25	0.01

Table 1: Model parameters of the two-piece double exponential model.

In Table 1, we list the model parameters of the two-piece double exponential model used in our numerical examples. Both sets of parameters are calibrated to the DAX implied volatility on 5 July, 2002. The first set of parameters [taken from Sepp (2004)] are calibrated to options with the shortest maturity (2 weeks or 0.04 year), while the second set [from Sepp and Skachkov (2003)] are calibrated to options with medium-term maturity (6 months or 0.5 year). In our numerical calculations, we take the change point to be at $t = 0.05$ (shown in Table 1).

Correspondingly, the moment generating function of $\ln \frac{S_t}{S_0}$ is a piecewise function, where

$$e^{\psi_t(u)} = \exp \left\{ t(r-d)u + \min\{t, t_0\} \left[\frac{\sigma^2}{2}(u^2 - u) + \lambda u \left(\frac{p}{\eta_+ - u} - \frac{1-p}{\eta_- + u} - m \right) \right] \right. \\ \left. + (t - t_0)^+ \left[\frac{\tilde{\sigma}^2}{2}(u^2 - u) + \tilde{\lambda} u \left(\frac{\tilde{p}}{\tilde{\eta}_+ - u} - \frac{1-\tilde{p}}{\tilde{\eta}_- + u} - \tilde{m} \right) \right] \right\},$$

for $-\min(\eta_-, \tilde{\eta}_-) < u < \min(\eta_+, \tilde{\eta}_+)$. The corresponding Lévy measure in each piece is given by $\lambda f_Y(x) dx$, where

$$f_Y(x) = p\eta_+ e^{-\eta_+ x} \mathbf{1}_{\{x \geq 0\}} + (1-p)\eta_- e^{\eta_- x} \mathbf{1}_{\{x < 0\}}.$$

For simplicity, we choose $r = d = 0$ and $S_0 = 1$ in our sample calculations.

Variance swaps

Suppose the evaluation time $t \in (t_{k-1}, t_k]$, where k is fixed. The value of a variance swap with strike K_V is given by

$$\mathbb{V}_t(0, T; M) = \frac{1}{T} \left\{ \sum_{i=1}^{k-1} \left(\ln \frac{S_{t_i}}{S_{t_{i-1}}} \right)^2 + \left(\ln \frac{S_t}{S_{t_{k-1}}} + \psi'_{t, t_k}(0) \right)^2 + \psi''_{t, t_k}(0) \right. \\ \left. + \sum_{i=k+1}^M \left[(\psi'_{t_{i-1}, t_i}(0))^2 + \psi''_{t_{i-1}, t_i}(0) \right] \right\} - K_V. \quad (4.2)$$

One can compute its delta and gamma readily by the following formulas:

$$\Delta_V = \frac{1}{T} \frac{2}{S_t} \left(\ln \frac{S_t}{S_{t_{k-1}}} + \psi'_{t, t_k}(0) \right), \quad (4.3a)$$

$$\Gamma_V = \frac{1}{T} \frac{2}{S_t^2} \left(1 - \ln \frac{S_t}{S_{t_{k-1}}} - \psi'_{t, t_k}(0) \right). \quad (4.3b)$$

Since the calculation of the value of a variance swap essentially only involves the evaluation of the floating leg, we set the strike price K_V to be zero for convenience in all variance swap calculations reported below.

In Table 2, we show the comparison of the time- t value of a typical 3-month ($M = 60$) variance swap contract with daily sampling ($\Delta t = 1/252$) and zero strike as well as the greeks computed using our FFT algorithm with the exact values computed by analytical pricing formulas (4.3a, 4.3b). We take $t = \Delta t/2$ and $S_t = S_0 = 1$. The values of L and N (which are the corresponding number of X -grid points) chosen in our sample calculations are shown in the first and second columns in Table 2, respectively. Here, N is taken to be a power of 2

L	N	price	CPU time	delta		gamma	
				Eq. (3.12a)	Eq. (3.13a)	Eq. (3.12b)	Eq. (3.13b)
2	2^7	0.133523	2s	-0.115486	-0.115522	9.242968	9.133254
4	2^8	0.115984	5s	-0.002936	-0.002886	8.408088	8.408410
6	2^9	0.115723	15s	-0.001315	-0.001312	8.401562	8.400184
8	2^{10}	0.115721	56s	-0.001299	-0.001299	8.401300	8.400001
10	2^{11}	0.115721	214s	-0.001299	-0.001299	8.401299	8.400000
exact		0.115721		-0.001299	-0.001299	8.401299	8.401299

Table 2: The time- $\Delta t/2$ price and the corresponding greek values of a three-month ($M = 60$) daily sampled variance swap with zero strike price under the two-piece double exponential model.

for effective implementation of the FFT algorithms. Our numerical experiments demonstrate that a fixed value of L for all choices of N is inappropriate as this causes oscillation and instability to the numerical results. By choosing an increasing sequence for L as N increases, we manage to keep Δx and $\Delta \beta$ to be in par. That is, both Δx and $\Delta \beta$ are reduced to attain a more accurate discretization of the Fourier integrals. Unfortunately, such a procedure may implicitly force us to choose an unrealistic small value of L (like $L = 2$ when $N = 2^7$). This may cause significant truncation error, as demonstrated by the numerical results in the row of $L = 2$ and $N = 2^7$ in Table 2. The third column in Table 2 lists the numerical results of the time- $\Delta t/2$ price of the variance swap under the given two-piece double exponential model (parameter values are presented in Table 1) corresponding to an increasing number of X -grid points. We also record the CPU time required for the FFT calculations that were implemented with Matlab2011 under a 32-bit Windows 7 system. The CPU time roughly increases by 4-fold when we double the value of N . In the columns labelled “delta” and “gamma”, we present the respective hedge parameter values computed using direct differentiation of the Fourier integral [Eqs. (3.12a) and (3.12b)] and the finite difference formulas [Eqs. (3.13a) and (3.13b)], respectively. We observe the apparent convergence of the numerical results of the price function and its hedge parameters to the respective exact value (shown in the last row). However, one has to be alerted that N must be chosen to be sufficiently large ($N \geq 2^8$ in our sample calculations) in order to achieve a reliable approximation to the exact value, especially in the calculations of delta and gamma values.

Variance options, volatility swaps and capped variance swaps

We now apply our FFT algorithm to pricing and hedging nonlinear contingent claims on the discretely sampled realized variance, namely, variance options, volatility swaps (volatility is the positive square root of the realized variance) and capped variance swaps. Note that the payoff of a put option on discretely sampled realized variance falls to a low value at very high

or low underlying asset price since the discretely sampled realized variance would achieve a high value under this scenario. This phenomenon is desirable in our implementation of the numerical algorithm since the truncation in the log asset price beyond a sufficiently large value of L would hardly cause any substantial error. For the calculation of the value of a call option on discretely sampled realized variance, one can employ the well known put-call parity relation to deduce the call value from the corresponding put value. For a volatility swap or a capped variance swap, the growth rate of its value is apparently limited by that of a variance swap at the extreme values of the underlying asset price. Therefore, our algorithm should not face any difficulty to deal with these swap products as long as the algorithm performs well for variance swaps. As a remark, choosing proper values for the parameters in the numerical scheme in the implementation procedure is of vital importance. From our experience in pricing variance swaps, we observe that $L = 6$ and $N = 2^9$ represent an appropriate set of parameters to ensure sufficient accuracy of the numerical results.

Discretization error of the quadratic variation approximation

It is known that accuracy of the quadratic variation approximation deteriorates for short-dated options on realized variance. Keller-Ressel and Muhle-Karbe (2010) have successfully quantified the discretization error using their asymptotic approximation method and confirm that the discretization effect cannot be ignored for short-dated options on realized variance when the underlying model has nonzero diffusion term. In Table 3, we present the numerical values of prices of various at-the-money put options, volatility swaps and capped variance swaps based on daily sampled realized variance obtained from our FFT algorithm and Monte Carlo simulation. We also include the approximate prices obtained based on quadratic variation against number of days to maturity. The range of maturity covers from one week (5 trading days) to three months (60 trading days). Like in our earlier pricing of variance swaps, we set the strikes of the volatility swaps K_w and capped variance swaps K_c to be zero for convenience. We computed the prices of the put options based on quadratic variation using the saddle-point approximation formula in Zheng and Kwok (2013b). On the other hand, the prices of the volatility swaps based on quadratic variation are computed by the numerical quadrature method. For the capped variance swaps, the terminal payoff defined in Eq. (2.6c) can be rewritten as

$$V(0, T; M) - K_c - \max(V(0, T; M) - C, 0). \quad (4.4b)$$

In other words, the terminal payoff of the capped variance swap is equal to that of its non-capped counterpart plus a short position of an out-of-the-money call on the realized variance with strike C . Thus, the prices of the capped variance swaps based on quadratic variation can be computed similarly as those for the put options. Since our goal is to compare the performance of the quadratic variation approximation for at-the-money put options, it is necessary to set different values of K_p for put options with differing maturities (note that different choices

of K_p represent different put options). The Monte Carlo simulation results are also presented in Table 3 as benchmark comparisons.

From Table 3, we observe the significant discretization error arising from the quadratic variation approximation for short-dated (5 days) put options on the daily sampled realized variance, though the discretization errors become smaller for put options with longer maturities. Similar properties on discretization errors are observed for short-dated volatility swaps. For capped variance swaps, the discretization error is not as substantial as those in put options or volatility swaps. Intuitively, though the cap introduces some degree of nonlinearity in the terminal payoff of the variance swap, the capped variance swap still resembles closely its non-capped counterpart under normal market conditions. In fact, we deduce from Eq. (4.4b) that under normal market conditions the deep-out-of-the-money call contributes very little to the overall value of the capped variance swap. Our calculations illustrate that poor accuracy of the quadratic variation approximation is common among nonlinear contingent claims on discretely sampled realized variance with short maturities.

maturity (days)		5	15	20	40	60
put option	K_p	0.161800	0.152741	0.140850	0.123014	0.117069
	MC	0.072538	0.063682	0.062796	0.059806	0.057037
	FT	0.072781	0.063628	0.062608	0.059730	0.057144
	QV	0.067528	0.062739	0.062158	0.059472	0.056941
volatility swap ($K_w = 0$)	MC	0.323547	0.331815	0.314073	0.288844	0.283305
	FT	0.323247	0.331801	0.313866	0.288786	0.283209
	QV	0.337483	0.336619	0.317506	0.290531	0.284315
capped variance swap ($K_c = 0$)	C	0.323600	0.305482	0.281700	0.246028	0.234138
	MC	0.100589	0.101587	0.090180	0.076021	0.073866
	FT	0.100517	0.101912	0.090353	0.076007	0.073735
	QV	0.101409	0.102233	0.090682	0.076382	0.074175

Table 3: The prices of various at-the-money put options, volatility swaps and capped variance swaps based on the daily sampled realized variance calculated by the Fourier transform algorithm (labelled “FT”) are compared to those obtained using quadratic variation approximation (labelled “QV”). The cap level C in the capped variance swap is chosen to be $2K_p$, where K_p is the at-the-money strike. The numerical results obtained by Monte Carlo simulation (labelled “MC”) using 10^5 simulation paths are seen to agree favorably well with those of the FFT calculations.

Calculations of prices and hedge parameters

While options on the quadratic variation have no direct dependence on the spot value of the

underlying asset price, it is not true for their discretely sampled realized variance counterparts when the valuation time is not at the initiation time. Consequently, it is useful to compute the delta and gamma of these products for hedging purposes. In our calculations, we assume the valuation time to be $\Delta t/2$, which lies in the middle of the first and second monitoring dates. We would like to investigate the properties of the hedge parameters of a typical one-month (20-day) put option on daily sampled realized variance. Figures 2(a,b,c) show the plots of the price, delta and gamma of the put option versus the spot price S_t . The price of the put option versus the spot price exhibits a bell shape. First, consider the scenario where $S_t = S_0$, the next squared return to be accumulated is expected to be the smallest among all scenarios. This would lead to the smallest expected realized variance, so the highest value for the put option price is resulted. On the other hand, when S_t is far away from S_0 , a larger squared return is expected to be accumulated. This then drives the put option price down to a smaller value. When the spot price S_t is less than the initial stock price S_0 , the delta value stays positive. This deduced result confirms well with the plot of the price function against S_t in Figure 2(a). The opposite effect on the delta value holds when the spot price is larger than S_0 . However, when the spot price is sufficiently far away from S_0 , the put option is bound to be out-of-the-money at maturity and any small change in the spot price will have little effect on the option price. As a result, the delta value is close to zero at the two ends far from S_0 . Moreover, since gamma is the rate of change of delta with respect to the spot value, the curvature pattern in the plot of gamma against S_t in Figure 2(c) can be fully inferred from the plot of delta in Figure 2(b). Note that the minimum value of gamma is realized when $S_t = S_0$ at which the gamma is negative, indicating that any significant change in the spot price will be unfavorable to the put option holder. We also observe good agreement between numerical results for the hedge parameters obtained using FFT calculations of the Fourier integral formulas [see Eqs. (3.12a, 3.12b)] and finite difference formulas [see Eqs. (3.13a, 3.13b)].

Choice of the Z-grid

Lastly, we would like to illustrate the vital importance of the choice of the Z -grid for the convergence of the numerical results in our FFT algorithms. In Table 4, we present the numerical results obtained using different choices of the distribution of Z -grid points. In the first column, an increasing sequence of the number of Z -grid points is presented. The numerical values of the price of a one-month (20-day) put option using the uniform Z -grid are shown in the second column with increasing value of K . The third and fourth columns show similar numerical values of the put option price obtained based on two nonuniform Z -grids that put more points on the left hand side of the range of Z . The graphic plots of the various choices of the distribution of the grid points are shown in Figure 1. The bottom row labelled “MC” presents the simulation results with 10^5 simulation paths as the benchmark. Note that the “nonuniform-2” grid is the best performer and it has been adopted in our previous calculations of option prices. It is disquieting to observe that the uniform Z -grid fails to give

any reasonable approximation value to the true price while the nonuniform-1 Z -grid exhibits oscillations around the true value.

K	uniform	nonuniform-1	nonuniform-2
2^6	0.138473	0.076182	0.060856
2^7	0.138232	0.067148	0.062276
2^8	0.137756	0.060535	0.062601
MC	0.062638	0.062638	0.062638

Table 4: The numerical results of the price of the one-month at-the-money put option under the two-piece double exponential model computed using different choices of Z -grid distribution and number of Z -grid points, K . In particular, $L = 6$ and $N = 2^9$ are fixed in the FFT calculations.

Downside variance swaps

We apply our FFT algorithms to price the downside variance swaps, whose product nature and some of its intriguing pricing properties have been discussed in Zheng and Kwok (2013a). Despite the slight difference between the generalized realized variance and realized variance with no restriction, we can handle the generalized variance swaps in a similar manner by modifying the state variable Z in the numerical algorithm accordingly. Numerical tests show that both the variance swaps and downside variance swaps are insensitive to the degree of fine resolution in the Z -grid due to linearity in Z in the payoff structure. We may simply choose a two-point grid of Z and use linear interpolation for other points.

L	N	$U = 0.9$	$U = 1$	$U = 1.1$	CPU time
2	2^7	0.075308	0.096388	0.113789	1s
4	2^8	0.071206	0.092287	0.109687	4s
6	2^9	0.071396	0.091777	0.109439	13s
8	2^{10}	0.070640	0.091325	0.109233	47s
10	2^{11}	0.070704	0.090987	0.108970	181s
	exact	0.070746	0.090419	0.108804	

Table 5: The numerical results of the time- $\Delta t/2$ price of the three-month daily sampled downside variance swap with zero strike price under the two-piece double exponential model are listed with varying values of the upper barrier U . The convergence of the numerical swap values to the exact values with increasing value of N is apparent, though the rate of convergence appears to be relatively slow. The last column presents the CPU time required for the FFT calculations for varying values of N and L .

In Table 5, we show the comparison of the price at time $\Delta t/2$ computed using our Fourier

transform algorithms of various three-month (60-day) downside variance swaps with varying values of the upper barrier U and explore the convergence to the respective exact value. Again, we take $S_0 = 1$ and set the strike price $K_d = 0$ for convenience. Similar to the variance swaps, apparent convergence to the exact values with increasing value of N is observed. For the downside variance swap with $U < 1$, we observe oscillation of the prices around the true value as N increases.

Next, we focus on the examination of the pricing properties of the downside variance swap with $U = 1.1$ and $S_0 = 1$. In particular, we examine how the price as well as the hedge parameters change with respect to the spot price of the underlying asset. In Figures 3(a,b,c), we show the plots of the prices of the downside variance swap and its greeks with varying values of the spot price. When S_t is less than S_0 , the price of the downside variance swap tends to decrease as S_t increases since the squared return to be accumulated is expected to decrease as a result. When S_t is above S_0 , the price of the downside variance swap first increases in value as S_t does, like the variance swap. However, this trend cannot persist since we have the upper barrier U (in this example, U is chosen to be slightly larger than S_0). In fact, when S_t approaches U , the probability that the squared return will not be accumulated increases rapidly due to the violation of the corridor restriction of the underlying asset price. When S_t comes closer to U , this ‘knock-out’ effect becomes more dominant and drives down the price of the downside variance swap. The plot of the time- $\Delta t/2$ price of the downside variance swap against S_t [shown in Figure 3(a)] agrees with the above intuitive arguments on the pricing properties. For the greeks, the numerical results obtained using FFT calculations of the Fourier integral formulas and finite difference formulas again show good agreement. The deviation becomes slightly larger at the spot price that is far away from S_0 [see Figures 3(b,c)]. At low values of S_t , the delta is negative and increases in value until it becomes close to zero at $S_t = S_0$. It then changes sign when S_t increases beyond S_0 . Interestingly, the delta value starts to drop as the ‘knock-out’ effect becomes more significant, consistent with the earlier discussion on the price function. It reaches a local minimum at $S_t = U$, at which the price of the downside variance swap is extremely sensitive to the spot price. When S_t is close to the upper barrier U , hedging of the downside variance swap becomes more difficult. This is a phenomenon that is commonly shared by derivatives with an embedded barrier feature. Any further increase in the spot price would cause less dramatic drop in the price of the downside variance swap. This is easily seen since when S_t is sufficiently large, ‘knock-out’ is almost sure to happen. This explains why the delta value asymptotically approaches zero from below [see Figure 3(b)]. Lastly, the plot of the gamma value in Figure 3(c) can be well inferred from that of the delta. The gamma value exhibits a high level of oscillation when S_t stays close to the upper barrier U .

5 Conclusion

We illustrate how to develop and apply effective fast Fourier transform algorithms for calculating the price functions and their hedge parameters of exotic variance and volatility derivatives on discretely sampled realized variance under time-inhomogeneous Lévy models (additive processes). We adopt the efficient procedure in the CONV method in the FFT calculations through expressing the price function as a convolution integral. Our enhanced Fourier transform algorithms represent non-trivial extension to the Fourier space time stepping algorithm. We show how special precautions have to be taken in order to incorporate the exotic path dependence associated with updating of the discretely sampled realized variance across discrete monitoring dates. Also, we illustrate how to perform truncation of the computational domain in order to avoid unboundedness of the solution values at the far ends of the computational domain and choose a nonuniform set of grids for the path dependent variable of the running average of squared returns. The usual difficulties in computing the hedge parameters in most option pricing algorithms can be resolved under FFT calculations. The efficiency, accuracy, reliability and robustness of our FFT algorithms are demonstrated through various numerical tests in pricing different types of exotic variance products and volatility derivatives. Lastly, we explore various properties of the price functions and their hedge parameters of put options on realized variance, volatility swaps, capped variance swaps and downside variance swaps. For future works, one may consider the extension to pricing more exotic path dependent variance products, like the timer options and target volatility options. One also explores how to deal with pricing under other types of asset price models, like the stochastic volatility model with jumps and time-changed Lévy processes.

ACKNOWLEDGEMENT

This research was supported by the Hong Kong Research Grants Council under Project 642110 of the General Research Funds.

REFERENCES

- Bernard, C., and Cui, Z. (2012). Prices and asymptotics for discrete variance swaps. Working paper of University of Waterloo.
- Broadie, M., and Jain, A. (2008). The effect of jumps and discrete sampling on volatility and variance swaps. *International Journal of Theoretical and Applied Finance*, **11(8)**, 761-797.
- Carr, P., Geman, H., Madan, D., and Yor, M. (2005). Pricing options on realized variance. *Finance and Stochastics*, **9**, 453-475.
- Carr, P., and Lee, R. (2009). Volatility derivatives. *Annual Review of Financial Economics*, **1**, 319-339.
- Carr, P., Lee, R., and Wu, L. (2012). Variance swaps on time-changed Lévy processes. *Finance and Stochastics*, **16**, 335-355.
- Carr, P., and Madan, D. (1998). Towards a theory of volatility trading. *Volatility*, edited by Jarrow, R., Risk Publications, London.
- Carr, P., and Wu, L. (2004). Time-changed Levy processes and option pricing. *Journal of Financial Economics*, **71**, 113-141.
- Carr, P., Geman, H., Madan, D., and Yor, M. (2005). Pricing options on realized variance. *Finance and Stochastics*, **9(4)**, 453-475.
- Cont, R., and Tankov, P. (2003). *Financial Modelling with Jump Processes*, Chapman and Hall/CRC, London.
- Crosby, J., and Davis, M. (2011). Variance derivatives: pricing and convergence. Working paper of University of Glasgow and Imperial College.
- Drimus, G.G. (2012). Options on realized variance by transform methods: a non-affine stochastic volatility model. *Quantitative Finance*, **12(11)**, 1679-1694.
- Dupire, B. (1993). Model art. *Risk*, September issue, 118-120.
- Fang, F., and Oosterlee, C.W. (2011). A Fourier-based valuation method for Bermudan and barrier options under Heston's model. *SIAM Journal of Financial Mathematics*, **2**, 439-463.
- Itkin, A., and Carr, P. (2010). Pricing swaps and options on quadratic variation under stochastic time change models - discrete observations. *Review of Derivatives Research*, **13**, 141-176.
- Jackson, K.R., Jaimungal, S., and Surkov, V. (2008). Fourier space time-stepping for option pricing with Lévy models. *Journal of Computational Finance*, **12(2)**, 1-29.

- Jarrow, R., Kchia, Y., Larsson, M., and Protter, P. (2011). Discretely sampled variance and volatility swaps versus their continuous approximations. Working paper of Cornell University.
- Kallsen, J., and Muhle-Karbe, J., and Voß, M. (2011). Pricing options on variance in affine stochastic volatility models. *Mathematical Finance*, **21(4)**, 627-641.
- Keller-Ressel, M., and Muhle-Karbe, J. (2010). Asymptotic and exact pricing of options on variance. Working paper of ETH, Zürich.
- Kwok, Y.K., Leung, K.S., and Wong, H.Y. (2012). Efficient options pricing using the fast Fourier transform. *Handbook of Computational Finance*, edited by Duan, J.C., Hardle, W.K., and Gentle, J.E., Chapter 21, 579-604, Springer, Berlin.
- Little, T., and Pant, V. (2001). A finite-difference method for the valuation of variance swaps. *Journal of Computational Finance*, **5(1)**, 81-103.
- Lord, R., Fang, F., Bervoets, F., and Oosterlee, C.W. (2008). A fast and accurate FFT-based method for pricing early-exercise options under Lévy processes. *SIAM Journal on Scientific Computing*, **30**, 1678-1705.
- Neuberger, A. (1994). The log contract. *Journal of Portfolio Management*, **20**, 74-80.
- Sepp, A., and Skachkov, I. (2003). Option pricing with jumps. *Wilmott Magazine*, November issue, 50-58.
- Sepp, A. (2004). Analytic pricing of double-barrier options under a double-exponential jump diffusion process: Applications of Laplace transform. *International Journal of Theoretical and Applied Finance*, **7(2)**, 151-175.
- Sepp, A. (2008). Pricing options on realized variance in the Heston model with jumps in returns and volatility. *Journal of Computational Finance*, **11(4)**, 33-70.
- Sepp, A. (2012). Pricing options on realized variance in the Heston model with jumps in returns and volatility II: an approximate distribution of the discrete variance. To appear in *Journal of Computational Finance*.
- Windcliff, H., Forsyth, P.A., and Vetzal, K.R. (2006). Pricing methods and hedging strategies for volatility derivatives. *Journal of Banking and Finance*, **30**, 409-431.
- Zheng, W.D., and Kwok, Y.K. (2013a). Closed form pricing formulas for discretely sampled generalized variance swaps. To appear in *Mathematical Finance*.
- Zheng, W.D., and Kwok, Y.K. (2013b). Saddlepoint approximation methods for pricing derivatives on discretely sampled realized variance. Working paper of Hong Kong University of Science and Technology.

Zhu, S.P., and Lian, G.H. (2011). A closed-form exact solution for pricing variance swaps with stochastic volatility. *Mathematical Finance*, **21(2)**, 233-256.

Zhylyevskyy, O. (2012). A fast Fourier transform technique for pricing American options under stochastic volatility. *Review of Derivatives Research*, **13**, 1-24.

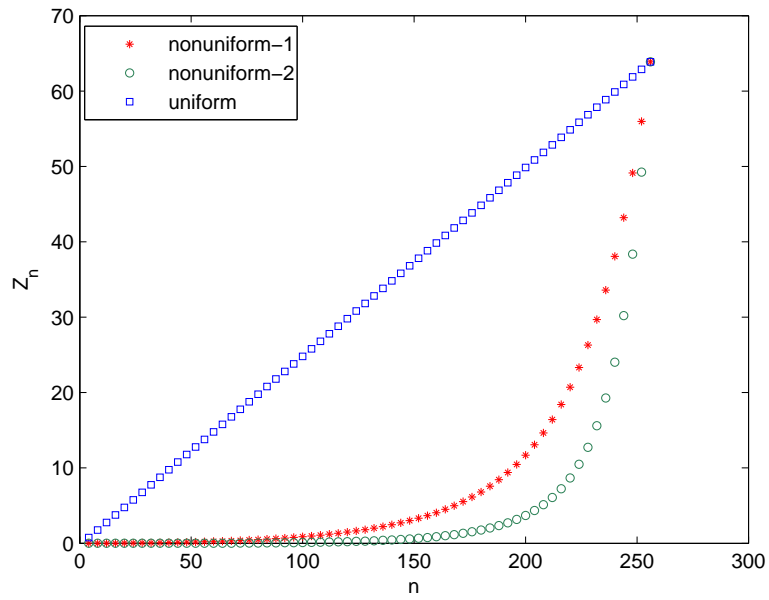


Figure 1: Plots of uniform and nonuniform Z -grids that are adopted for pricing put options on discretely sampled realized variance. Here, n is the running index for the Z -grid points. The plots indicate that more points are allocated to the left sides of the Z -range under nonuniform-2.

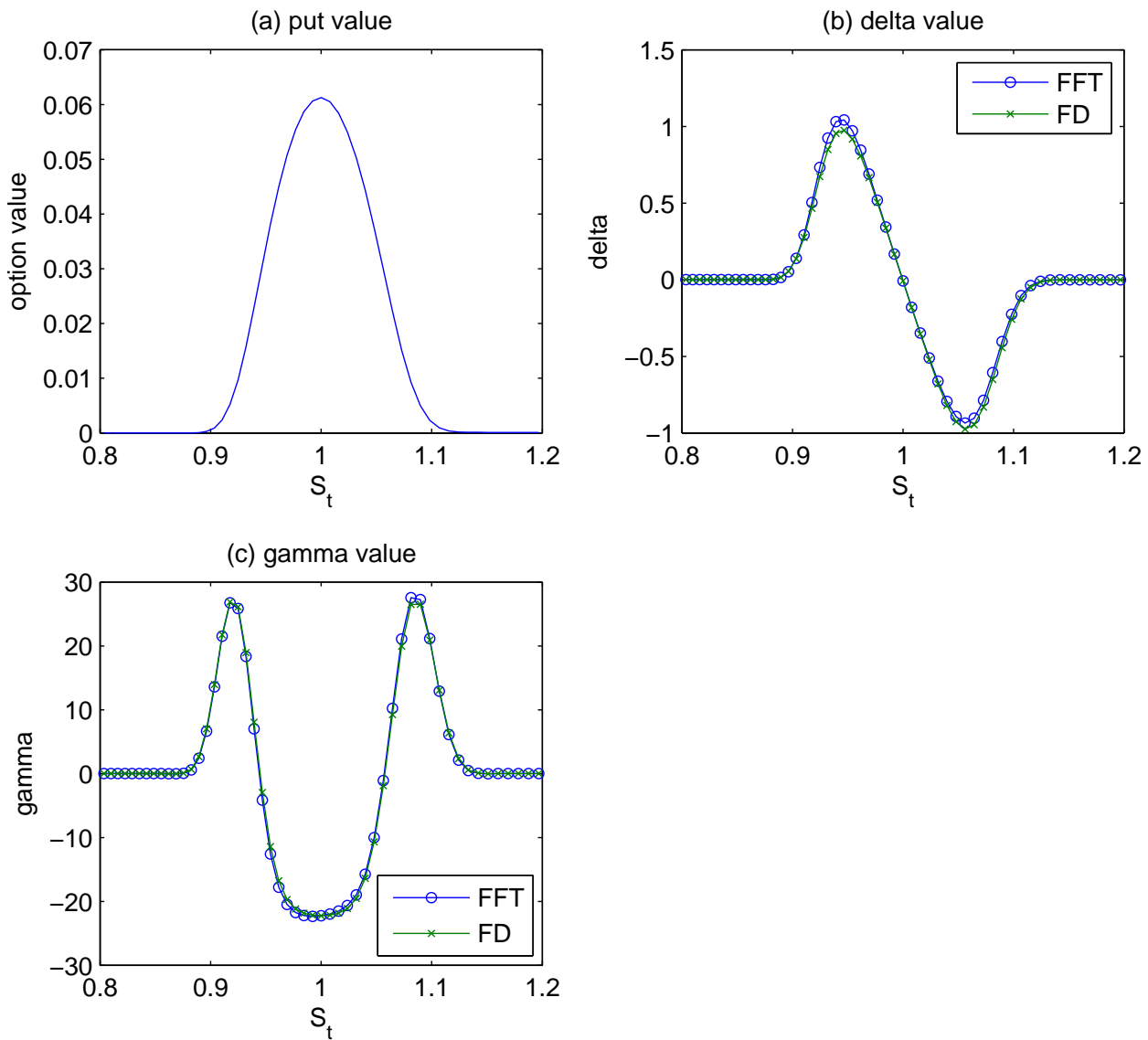


Figure 2: Plots of the option value, delta and gamma of the one-month put option on daily sampled realized variance at valuation time $\Delta t/2$ versus the spot price S_t . Good agreement between the numerical results on the delta and gamma obtained using FFT calculations of the Fourier integral formulas (labelled “FFT”) and finite difference formulas (labelled “FD”) is observed.

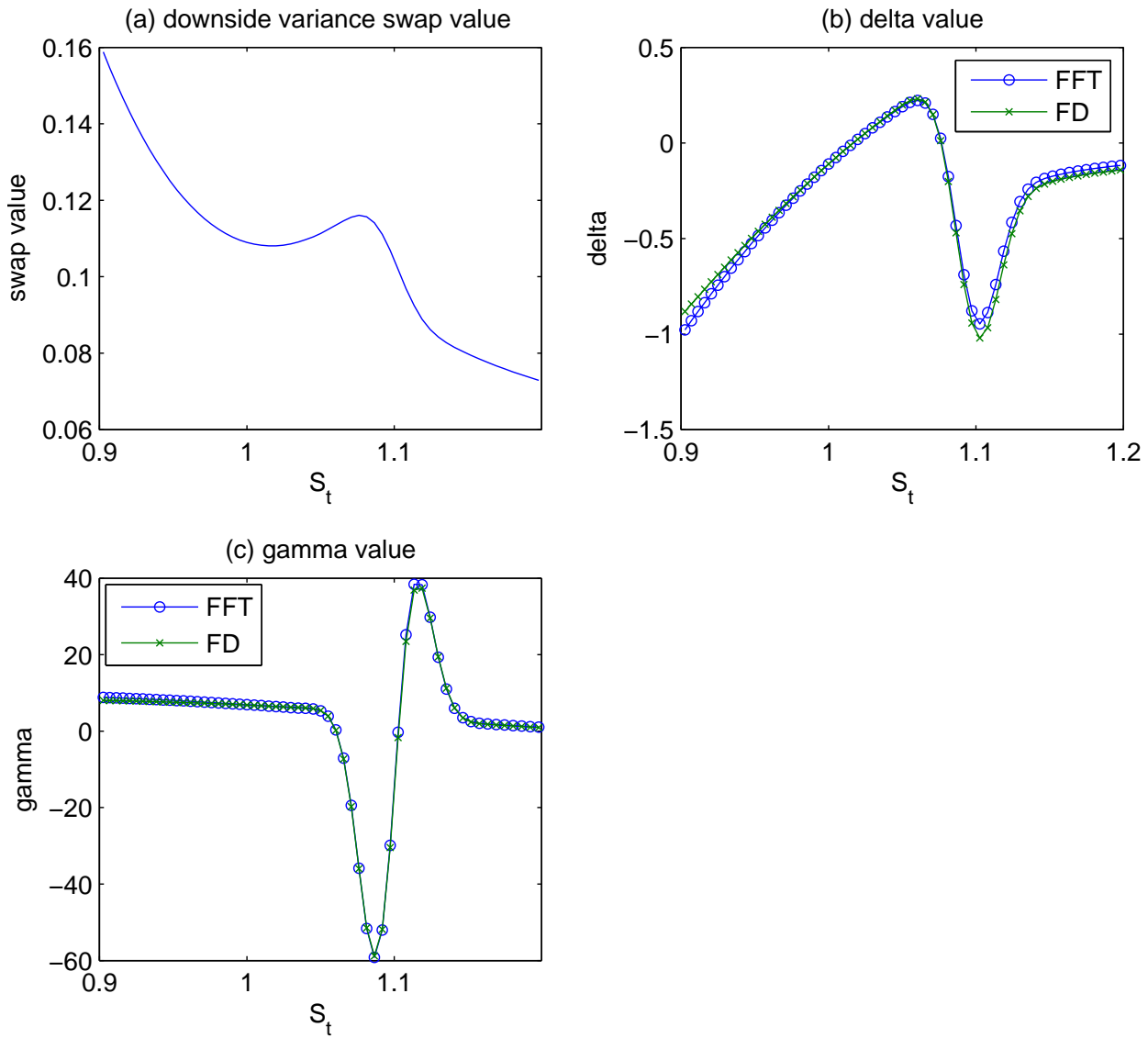


Figure 3: Plots of the swap value, delta and gamma of the three-month daily sampled downside-variance swap with $U = 1.1$ at valuation time $\Delta t/2$ versus the spot price S_t . Good agreement between the numerical results on the delta and gamma obtained using FFT calculations of the Fourier integral formulas (labelled “FFT”) and finite difference formulas (labelled “FD”) is observed.